

# Differential Effects of Surfactant Protein A on Regional Organization of Phospholipid Monolayers Containing Surfactant Protein B or C

Svetla G. Taneva\* and Kevin M. W. Keough\*†

\*Department of Biochemistry and †Discipline of Pediatrics, Memorial University of Newfoundland, St. John's, Newfoundland A1B 3X9, Canada

**ABSTRACT** Epifluorescence microscopy combined with a surface balance was used to study monolayers of dipalmitoylphosphatidylcholine (DPPC)/egg phosphatidylglycerol (PG) (8:2, mol/mol) plus 17 wt % SP-B or SP-C spread on subphases containing SP-A in the presence or absence of 5 mM  $\text{Ca}^{2+}$ . Independently of the presence of  $\text{Ca}^{2+}$  in the subphase, SP-A at a bulk concentration of 0.68  $\mu\text{g/ml}$  adsorbed into the spread monolayers and caused an increase in the molecular areas in the films. Films of DPPC/PG formed on SP-A solutions showed a pressure-dependent coexistence of liquid-condensed (LC) and liquid-expanded (LE) phases. Apart from these surface phases, a probe-excluding phase, likely enriched in SP-A, was seen in the films between  $7 \text{ mN/m} \leq \pi \leq 20 \text{ mN/m}$ . In monolayers of SP-B/(DPPC/PG) spread on SP-A, regardless of the presence of calcium ions, large clusters of a probe-excluding phase, different from probe-excluding lipid LC phase, appeared and segregated from the LE phase at near-zero surface pressures and coexisted with the conventional LE and LC phases up to  $\sim 35 \text{ mN/m}$ . Varying the levels of either SP-A or SP-B in films of SP-B/SP-A/(DPPC/PG) revealed that the formation of the probe-excluding clusters distinctive for the quaternary films was influenced by the two proteins. Concanavalin A in the subphase could not replace SP-A in its ability to modulate the textures of films of SP-B/(DPPC/PG). In films of SP-C/SP-A/(DPPC/PG), in the absence of calcium, regions consisting of a probe-excluding phase, likely enriched in SP-A, were detected at surface pressures between 2 mN/m and 20 mN/m in addition to the lipid LE and LC phases.  $\text{Ca}^{2+}$  in the subphase appeared to disperse this phase into tiny probe-excluding particles, likely comprising  $\text{Ca}^{2+}$ -aggregated SP-A. Despite their strikingly different morphologies, the films of DPPC/PG that contained combinations of SP-B/SP-A or SP-C/SP-A displayed similar distributions of LC and LE phases with LC regions occupying a maximum of 20% of the total monolayer area. Combining SP-A and SP-B reorganized the morphology of monolayers composed of DPPC and PG in a  $\text{Ca}^{2+}$ -independent manner that led to the formation of a separate potentially protein-rich phase in the films.

## INTRODUCTION

Pulmonary surfactant is a surface-active material composed of phospholipids ( $\sim 90\%$ ) and proteins ( $\sim 5\text{--}10\%$ ) that lines the alveolar epithelium and contributes to the structural stability of the alveolus during respiration (Von Neergaard, 1929). This function is accomplished via the surface tension-reducing properties of the lipid-protein layer at the air-water interface in the alveoli (Clements et al., 1961). Surfactant protein A (SP-A) is the major pulmonary surfactant-associated protein by mass (King and Clements, 1972). It is a hydrophilic glycoprotein with monomeric molecular mass of 28–36 kDa and an isoelectric point ranging from 4.8 to 5.2 (Sueishi and Benson, 1981). SP-A is characterized by a collagen-like N-terminal domain and variable glycosylation of the C-terminal region (Hawgood et al., 1985). The latter has binding sites for

carbohydrates and calcium (Haagsman et al., 1987, 1990). Subunits of SP-A form trimers that associate into an octadecamer with a molecular mass of  $\sim 700 \text{ kDa}$  (King et al., 1989). SP-B is a homo-dimer of disulfide-linked 79-residue monomers ( $M_r = 17.4 \text{ kDa}$ ) which contains regions of amphipathic  $\alpha$ -helix and has a net charge of +12 (Curstedt et al., 1988). SP-C is a 35-amino acid residue protein that contains two thioester-linked palmitoyl groups giving a total molecular mass of 4.2 kDa. It has a 23-residue C-terminal  $\alpha$ -helical portion and also has a net charge of +3 associated with residues near its N-terminal region (Curstedt et al., 1990). SP-B and SP-C are hydrophobic proteins soluble in organic solvents.

Pulmonary surfactant, as isolated by centrifugation from endobronchial lavage fluid, is composed of several different morphological forms including tubular myelin, lamellar bodies, and large and small aggregates (Benson et al., 1984; Putman et al., 1996). Secreted into the alveolar hypophase by type II cells as lamellar bodies, pulmonary surfactant is transformed into tubular myelin that is thought to represent a reservoir for the surface layer at the air-alveolar interface (Gil and Reiss, 1973; Sen et al., 1988). SP-A has been localized immunocytochemically in the tubular myelin structure (Walker et al., 1986), and it is required together with SP-B to produce tubular myelin forms from DPPC, PG, and calcium, in vitro (Suzuki et al., 1989; Williams et al., 1991).

Received for publication 17 December 1999 and in final form 12 June 2000.

Address reprint requests to Dr. Kevin M. W. Keough, Department of Biochemistry, Memorial University of Newfoundland, St. John's, Newfoundland A1B 3X9, Canada. Tel.: 709-737-2530; Fax: 709-737-2552; E-mail: kkeough@morgan.ucs.mun.ca.

**Abbreviations used:** DPPC, 1,2-dipalmitoyl-*sn*-glycerophosphocholine; con A, concanavalin A; EDTA, ethylenediaminetetraacetic acid; HEPES, *N*-[2-hydroxyethyl]piperazine-*N'*-[2-ethanesulfonic acid]; NBD-PC, 1-palmitoyl-2-[12-[(7-nitro-2-1,3-benzoxadiazol-4-yl)amino]dodecanoyl]-*sn*-glycero-3-phosphocholine; PG, *L*- $\alpha$ -phosphatidylglycerol from egg-sodium salt; Tris-HCl, tris[hydroxymethyl]-aminomethane hydrochloride.

© 2000 by the Biophysical Society

0006-3495/00/10/2010/14 \$2.00

SP-A and SP-B have been shown to have cooperative, calcium-dependent effects on some properties of surfactant phospholipids. They enhanced the surface activity of phospholipid mixtures (Hawgood et al., 1987), improved the resistance of pulmonary surfactant to inhibition by blood and plasma proteins (Venkataraman et al., 1990), and promoted phospholipid membrane fusion (Poulain et al., 1992, 1996). These studies have suggested that interactions between SP-A and SP-B have a role in the structural organization and biophysical activity of pulmonary surfactant.

This study includes mixtures of phospholipids and proteins with particular ratios relevant to those used in reconstitution of tubular myelin *in vitro* (Suzuki et al., 1989; Williams et al., 1991). We have used monolayer models to study interactions of SP-A with DPPC/PG containing SP-B or SP-C in the presence or absence of calcium. DPPC is the major phospholipid (~40% of the total phospholipid) and PG is the major acidic phospholipid (up to 12% of the total phospholipid) in pulmonary surfactant (Yu et al., 1983). Epifluorescence microscopic examination of the lipid-protein monolayers provides evidence for association of SP-A and SP-B, and segregation of a protein-rich phase in the phospholipid films containing the combination of SP-A/SP-B. A similar SP-A/SP-B-separated phase may play a role in the assembly of tubular myelin *in vitro* and *in vivo* and could have an impact on film dynamics at the alveolar surface.

## MATERIALS AND METHODS

### Materials

DPPC, Tris-HCl, and EDTA were purchased from Sigma Chemical Co. (St. Louis, MO). NBD-PC and PG were obtained from Avanti Polar Lipids Inc. (Alabaster, AL), and sodium chloride, calcium chloride, reagent grade, from Fisher Scientific Co. (Ottawa, ON, Canada). DPPC and PG showed single bands on thin-layer chromatography on silica gel with a solvent system of chloroform-methanol-water (65:25:4 by volume) and were used without further purification. Concanavalin A-lissamine rhodamine B was obtained from Molecular Probes Inc. (Eugene, OR).

### Protein isolation

Pig lungs were lavaged with 0.15 M NaCl and the lavage was centrifuged at  $800 \times g$  for 10 min. The supernatant was centrifuged at  $7000 \times g$  for 60 min. The pellet was used for isolation of either SP-A or SP-B and SP-C. SP-A was purified from the surfactant pellet by extraction with 1-butanol (Haagsman et al., 1987; Taneva et al., 1995). SDS-polyacrylamide gel electrophoresis (12% gel) was performed on samples of SP-A solutions according to the method of Laemmli (1970) followed by staining with Coomassie Blue. Under reducing conditions (5%  $\beta$ -mercaptoethanol in the sample buffer) a major band at ~36 kDa and a minor band at ~28 kDa were observed.

SP-B and SP-C were prepared from the surfactant pellet independently of the SP-A preparation as described previously (Curstedt et al., 1988; Taneva and Keough, 1995). SP-B and SP-C were separated from the surfactant lipids and each other by gel exclusion chromatography on Sephadex LH-60 (2.5  $\times$  90 cm) using chloroform/methanol (1:1, v/v) acidified with 2% by volume of 0.1 N HCl. On SDS-polyacrylamide gel

electrophoresis (16% gels) under non-reducing conditions, SP-B showed a major band at ~18 kDa and a minor one at ~29 kDa, whereas SP-C showed a single band at ~5 kDa. SP-B and SP-C were stored in chloroform/methanol (1:1, v/v).

### Analytical methods

Concentrations of SP-A, SP-B, and SP-C were estimated by the fluorescamine method using bovine serum albumin as a standard (Udenfriend et al., 1972). The concentration of SP-A was also determined from the absorbance of its solutions at 277 nm using an extinction coefficient determined by amino acid analysis of porcine SP-A. Quantitative amino acid analysis (Sarin et al., 1990) was used to verify the concentrations of SP-B and SP-C because the fluorescamine assay sometimes overestimated the concentrations of SP-C, possibly due to the presence of minor quantities of phospholipids containing primary amino groups, and because of compositional differences resulting in different fluorescamine reactivity between SP-C and albumin. Solutions of con A were prepared in 5 mM HEPES (pH 6.9) by weighing. Concentrations of DPPC, PG, and NBD-PC, dissolved in chloroform, were determined by measuring the phospholipid phosphorus (Bartlett, 1959; Keough and Kariel, 1987). Water used in all experiments and analytical procedures was deionized and doubly distilled in glass, the second distillation being from dilute potassium permanganate solution.

### Epifluorescence microscopy

Epifluorescence microscopy and surface pressure-area measurements were performed on a surface balance whose construction and operation have been described previously (Nag et al., 1990, 1991). The trough design, however, has been modified and now it has a continuous Teflon ribbon-barrier that prevents leakage of monolayer material. The lipids, DPPC and PG, and SP-B or SP-C were mixed in chloroform/methanol solutions and 1 mol % NBD-PC (based on the lipid content) was added. Monolayers were formed by spreading the mixtures of DPPC/PG (8:2, mol/mol) containing SP-B or SP-C on subphases of 145 mM NaCl, 5 mM Tris-HCl,  $\pm 5$  mM  $\text{CaCl}_2$  (pH 6.9) in the presence or absence of SP-A in the subphase. Tris buffer was used rather than phosphate or carbonate buffers because it does not precipitate  $\text{Ca}^{2+}$  salts. In experiments performed on SP-A-containing subphases, the surface of the protein solution in the Langmuir trough was swept clean by passing the barrier, and the lipid or lipid/SP-B or SP-C mixtures were spread on the newly formed surface. The initial spreading surface pressure was ~0 mN/m. After spreading, 60 min was allowed for adsorption of SP-A and equilibration of the monolayers; surface pressures of the films did not change  $>1$  mN/m during this period. Films were compressed in 30 steps at a rate of 20 mm<sup>2</sup>/s and isotherms of surface pressure ( $\pi$ ) versus monolayer area were recorded. At selected surface pressures monolayers were observed (40 $\times$  objective lens) through the fluorescence of NBD-PC, which partitions preferentially into the phospholipid fluid (LE) phase. Each experiment, performed at 22–24°C, took ~3 h. Usually 10 images at each surface pressure were analyzed with video analysis software (Jandel Scientific, Corte Madera, CA). The relative amount of probe-excluding liquid-condensed phase (% dark phase) was determined and plotted as a function of the surface pressure (Nag et al., 1991).

The monolayer area was determined as mean area per “residue,”  $A_{\text{mean}}$ , where a “residue” denotes one amino acid residue of hydrophobic protein (SP-B or SP-C) or one lipid molecule (DPPC and PG) ( $A_{\text{mean}} = \text{trough area}/(N_l + N_r)$ , where  $N_l$  and  $N_r$  denote the number of spread lipid molecules and amino acid residues of SP-B or SP-C). The concentrations of SP-B or SP-C in the spread lipid-protein monolayers were defined as weight percent of protein or “residue” fraction,  $X_r$ , of the protein amino acid residues calculated on the basis of molecules of lipids and amino acid

residues of protein spread initially in the monolayers (Taneva and Keough, 1994a).

## RESULTS

### Spread monolayers of DPPC/PG plus SP-B or SP-C formed on subphases containing SP-A in the absence of $\text{Ca}^{2+}$

Compression isotherms of surface pressure versus area for monolayers of DPPC/PG and those of SP-B/(DPPC/PG) or SP-C/(DPPC/PG) in the presence (*filled circles*) and the absence (*open circles*) of SP-A in the subphase (Fig. 1, *A* and *B*) were obtained. Monolayer area was expressed as mean area occupied by a lipid molecule or amino acid residue of hydrophobic protein (SP-B or SP-C) and therefore the contribution of SP-A adsorbed into the spread films to the monolayer area was not accounted for. In the whole range of surface pressures between 0 and  $\sim 45$  mN/m the adsorption of SP-A to the spread films led to an increase in their molecular areas compared to the values measured in the absence of SP-A (Fig. 1, *filled* and *open symbols*). The difference  $\Delta A$  occupied by a “residue” in the spread monolayers in the presence and absence of SP-A was determined at selected surface pressures for the three monolayer systems in Fig. 1. The relative expansion in the area due to the SP-A inserted into the spread films showed a maximum of 15–20% at  $\sim 20$  mN/m for the three systems, and this observation implied that SP-A was inserted to a similar extent into the spread films of different compositions. Based on the assumption that SP-A adsorbed into the spread monolayers occupied an area equal to that taken in the spread films of SP-A alone (Taneva et al., 1995), we used the area  $\Delta A$  to calculate the amount of SP-A incorporated into the films of DPPC/PG alone and DPPC/PG plus 17 wt % SP-B or SP-C spread on SP-A solutions at  $C_s = 0.68$   $\mu\text{g/ml}$ . The estimation showed that at  $\pi = 20$  mN/m each of the above spread films contained  $\sim 12$  wt % SP-A. SP-A

appeared to be inserted into the films of DPPC/PG and DPPC/PG plus SP-B (Fig. 1 *A*) or SP-C (Fig. 1 *B*) up to  $\pi = 40$ – $45$  mN/m, above which it apparently did not occupy area in the monolayer surface. Maximum surface pressures of  $\sim 45$  mN/m were achieved in the monolayers due to the relatively low compression rates and the stepwise compression used in this study.

Typical images seen at selected surface pressures in the monolayers of DPPC/PG spread on subphases without or with SP-A are shown in Fig. 2, *A* and *B*. At  $\pi \leq 5$  mN/m monolayers of DPPC/PG formed on subphases without SP-A existed in the homogeneously fluorescent liquid-expanded (LE) state (Fig. 2 *Aa*). Black probe-excluding domains of the liquid-condensed (LC) phase appeared at  $\pi \approx 6$  mN/m and grew in size with increasing surface pressure (*double arrowheads* in Fig. 2, *Ab–d*). The presence of SP-A in the subphase did not change the homogeneous appearance of the films at the low pressures (Fig. 2 *Ba*). However, the nucleation of the LC phase at  $\pi \approx 7$  mN/m appeared to enhance the adsorption of SP-A to the surface since the formation of the condensed domains caused the appearance of a grayish probe-excluding phase (Fig. 2 *Bb*) in addition to the probe-excluding LC domains (*double arrowheads* in Fig. 2, *Bb–d*). The LC phase in phospholipid films promotes the adsorption of SP-A to the surface (Ruano et al., 1998) and the appearance of the grayish phase in the DPPC/PG films spread on SP-A solutions, therefore, could be correlated with adsorption and accumulation of SP-A in the monolayer. The probe-excluding phase associated with SP-A adsorbed to the surface was seen up to  $\pi \approx 20$  mN/m, whereas at higher pressures typical LC domains (*double arrowheads* in Fig. 2, *Bc, d*) were distributed amid a brightly fluorescent background similar to the appearance of the films in the absence of SP-A (Fig. 2, *Ac, d*).

Images observed at selected surface pressures in films of DPPC/PG containing 17 wt % SP-B, spread on subphases without or with SP-A, are shown in Fig. 3, *A* and *B*. In the absence of SP-A in the subphase, dark circular probe-excluding domains were observed amid a fluorescent background in the protein-lipid films at low surface pressures (*small arrowheads* in Fig. 3 *Aa*). These structures seen in the SP-B/(DPPC/PG) films at surface pressures where the DPPC/PG films alone exist in the homogeneous LE state (Fig. 2 *Aa*) coexisted with the LE and LC phases up to  $\sim 20$  mN/m, where they were no longer detected. These protein-induced domains of circular shapes likely represented a form of a two-dimensional gas phase entrapped in the films compressed to surface pressures above the transition from gaseous to liquid expanded state. At  $\pi \approx 7$ – $8$  mN/m probe-excluding domains of irregular shapes, likely conventional LC phase, appeared and grew larger with a further increase in surface pressure (*double arrows* in Fig. 3, *Ab, c*).

Surface textures of SP-B/(DPPC/PG) monolayers significantly changed when SP-A was in the subphase (Fig. 3 *B*). Large grayish clusters of the probe-excluding phase (*large*

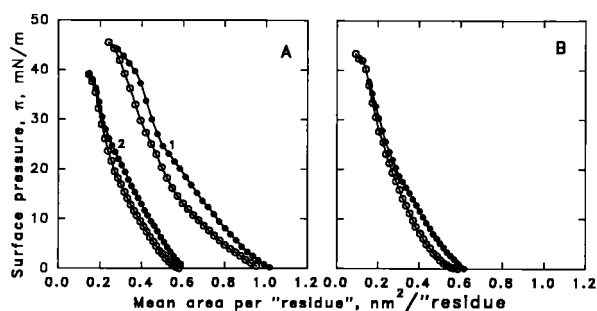


FIGURE 1 Isotherms of surface pressure versus mean area per “residue” for spread monolayers of (*A*) DPPC/PG (8:2, mol/mol) (1), DPPC/PG plus 17 wt % SP-B ( $X_r = 0.58$ ) (2), (*B*) DPPC/PG plus 17 wt % SP-C ( $X_r = 0.56$ ). Each monolayer contained 1 mol % (based on phospholipid content) of NBD-PC. The subphase was 145 mM NaCl, 5 mM Tris-HCl, 2 mM EDTA without (○) or with (●) 0.68  $\mu\text{g/ml}$  SP-A (pH 6.9).



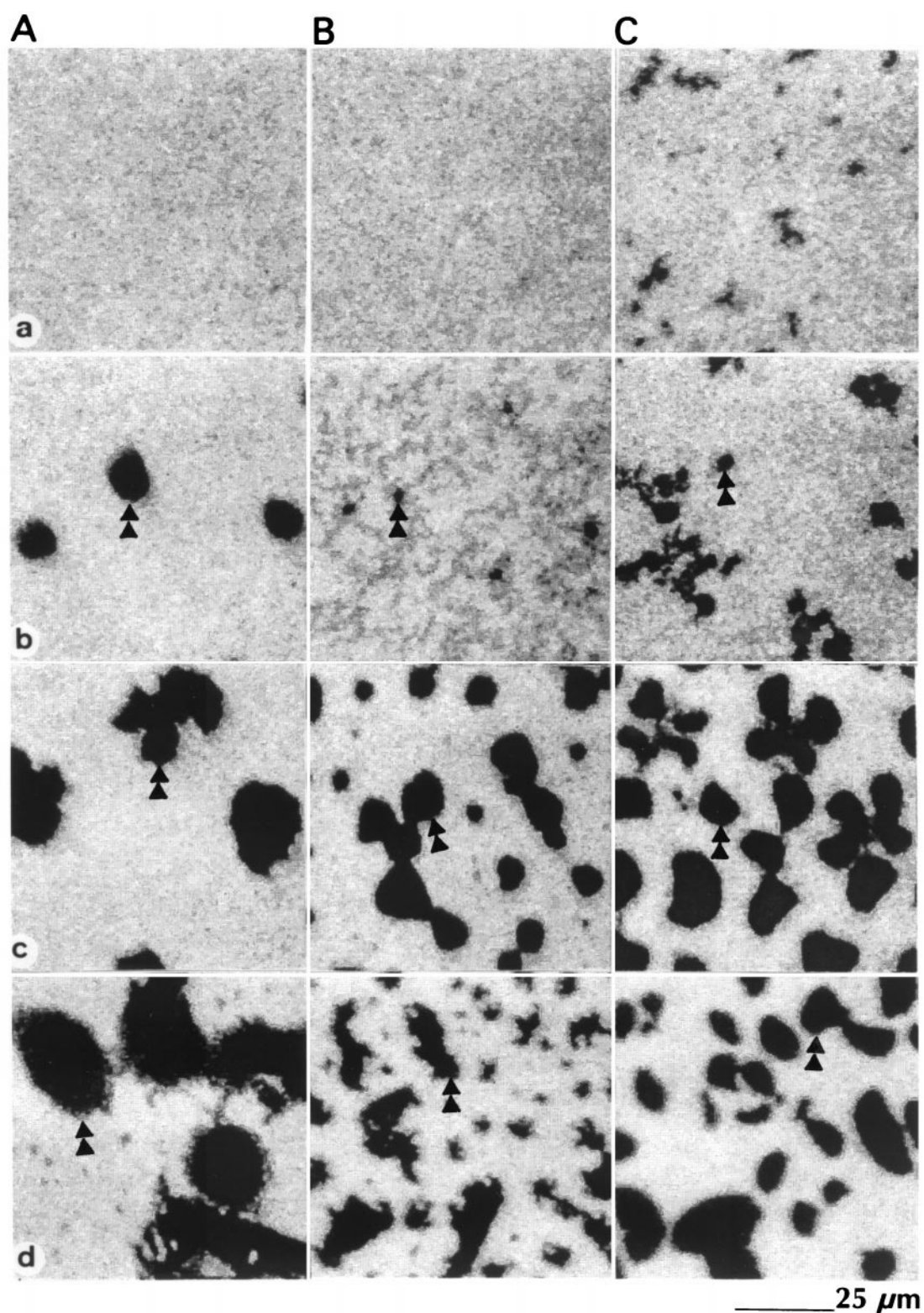


FIGURE 2 Epifluorescence micrographs of monolayers of DPPC/PG (8:2, mol/mol) at selected surface pressures 5 mN/m (*a*), 10 mN/m (*b*), 20 mN/m (*c*), and 35 mN/m (*d*). The subphase was 145 mM NaCl, 5 mM Tris-HCl (pH 6.9) plus 2 mM EDTA (*A*); plus 2 mM EDTA and 0.68 μg/ml SP-A (*B*); plus 5 mM CaCl<sub>2</sub> and 0.68 μg/ml SP-A (*C*). Double arrowheads indicate LC domains.

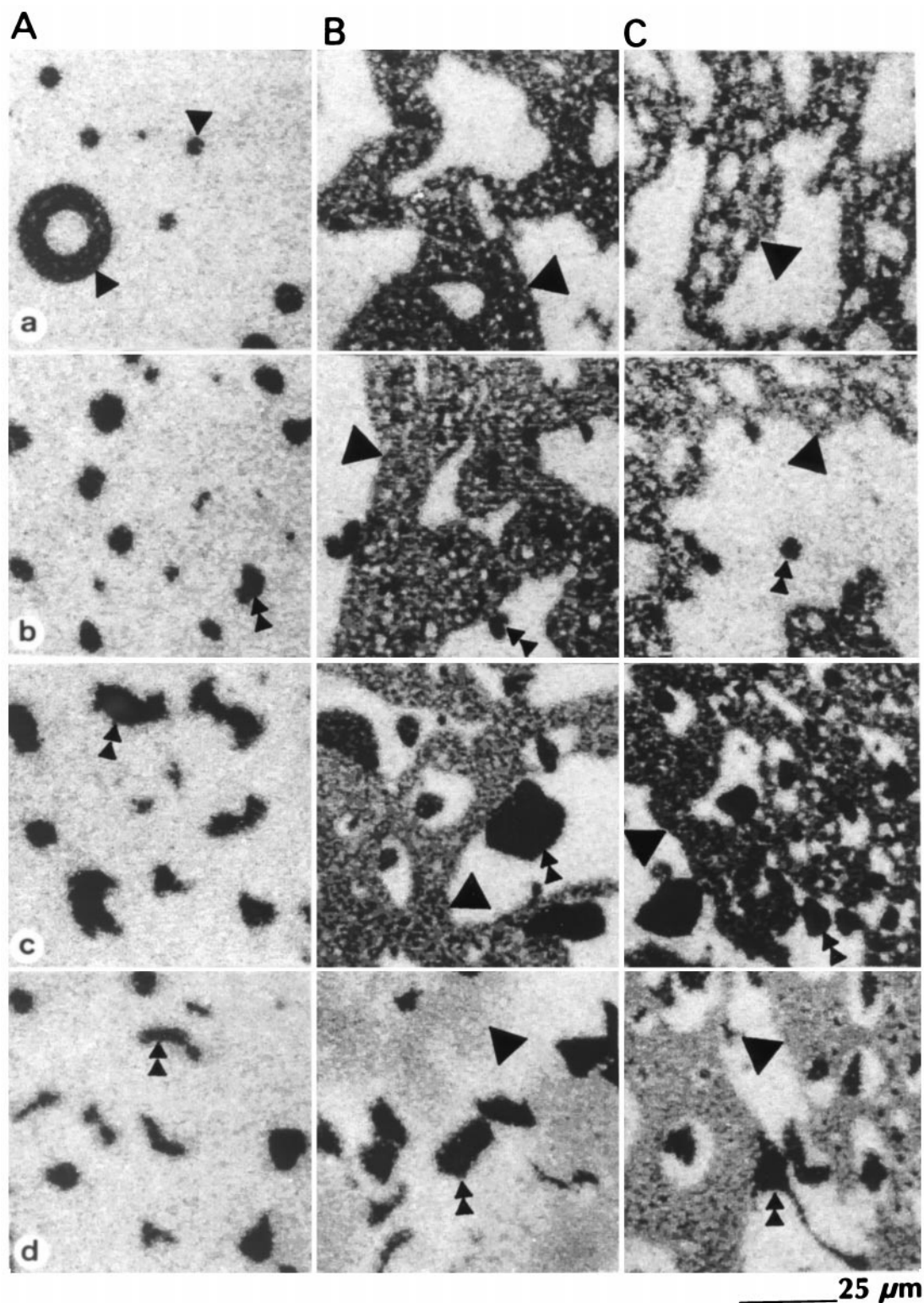


FIGURE 3 Epifluorescence micrographs of monolayers of DPPC/PG (8:2, mol/mol) plus 17 wt % SP-B ( $X_r = 0.58$ ) at a surface pressure of 5 mN/m (a), 10 mN/m (b), 20 mN/m (c), and 35 mN/m (d). The subphase was 145 mM NaCl, 5 mM Tris-HCl (pH 6.9) plus 2 mM EDTA (A); plus 2 mM EDTA and 0.68  $\mu\text{g/ml}$  SP-A (B); plus 5 mM  $\text{CaCl}_2$  and 0.68  $\mu\text{g/ml}$  SP-A (C). Small arrowheads indicate gaseous phase, double arrowheads LC domains, and large arrowheads SP-B/SP-A-rich phase segregated from lipid phases.



*arrowheads* in Fig. 3 *Ba*), which occupied  $52\% \pm 32\%$  (mean  $\pm$  SD, 10 images analyzed) from the total monolayer surface at  $\pi = 2.5$  mN/m, coexisted with the LE phase at low surface pressures. Small black circular domains, similar to those seen in the SP-B/(DPPC/PG) films in the absence of SP-A (*small arrowheads* in Fig. 3 *Aa*), were dispersed within this grayish phase. Note that at these low surface pressures the probe-excluding conventional lipid LC phase does not usually exist. At  $\pi \geq 8$  mN/m another kind of black probe-excluding domains (likely LC phase) nucleated and grew with surface pressure in the fluorescent LE phase both outside and within the clusters (*double arrowheads* in Fig. 3, *Bb*, *c*). The large probe-excluding clusters were faint but still discernible at the highest surface pressures measured in the films ( $\approx 40$  mN/m) (*large arrowheads* in Fig. 3 *Bd*).

Monolayers of SP-C/(DPPC/PG) spread on subphases without SP-A (Fig. 4 *A*) showed surface textures similar to those seen in the films of SP-B/(DPPC/PG) spread on SP-A-free subphases (Fig. 3 *A*). Dark circular probe-excluding domains were seen at the low surface pressures (*small arrowheads* in Fig. 4 *Aa*) and persisted up to  $\pi \approx 20$  mN/m. New probe-excluding domains, likely LC phase, nucleated at  $\pi \geq 7$ –8 mN/m and grew in size with increasing surface pressure (*double arrowheads* in Fig. 4, *Ab*, *c*). In the presence of SP-A in the subphase, at low surface pressures the grayish probe-excluding phase was present in the films of SP-C/(DPPC/PG) (Fig. 4, *Ba*, *b*) within which dark circular probe-excluding domains (*arrowheads* in Fig. 4 *Ba*) were seen. With increasing surface pressure the area occupied by this grayish phase diminished and was gradually replaced by a homogeneously fluorescent background, amid which LC domains were distributed (*double arrowheads* in Fig. 4 *Bb*–*d*). Remnants of the grayish phase were still seen at  $\pi \approx 20$  mN/m (Fig. 4 *Bc*).

Fig. 5 shows the relative area of the probe-excluding LC phase plotted as a function of surface pressure for films of DPPC/PG alone (*curve 1*) or supplemented with SP-B (*curve 2*) or SP-C (*curve 3*) spread on subphases containing SP-A. Note that the area of the large probe-excluding clusters seen in the films of SP-B/(DPPC/PG) spread on SP-A (*large arrowheads* in Fig. 3 *B*) was not included in the values of percent dark phase. In the films of DPPC/PG spread on SP-A maximal condensation of  $\sim 30\%$  was reached at  $\pi \approx 30$  mN/m. Relative areas of probe-excluding LC domains (*double arrowheads* in Figs. 3 *B* and 4 *B*) of  $\sim 20\%$  at  $\pi \approx 25$  mN/m were determined both for the films of DPPC/PG containing SP-B/SP-A (*curve 2*) and SP-C/SP-A (*curve 3*). The tendency of percent dark (LC) phase to decrease with surface pressure at  $\pi > 30$  mN/m could be related to a number of processes concurring at surface pressures  $\geq 30$  mN/m: 1) partial desorption of SP-A from the surface (Taneva et al., 1995); 2) onset of squeeze-out of SP-B or SP-C (Taneva and Keough, 1995); 3) onset of squeeze-out of PG (Boonman et al., 1987). It is likely that

along with the above components, which reside in the LE phase and leave the surface at  $\geq 30$  mN/m, some phospholipid from the edges of the LC domains was removed and this may account for the decrease in the relative proportions of the LC phase at these pressures (Fig. 5). The loss of edge tension-reducing components (i.e., the proteins) might also have changed the line tension at the liquid condensed liquid expanded phase boundary (Heckl et al., 1989).

The similarity between the plots of percent dark phase ( $\pi$ ) for the two lipid/protein films (*curves 2* and *3* in Fig. 5) revealed that the difference observed in the microscopic organization of the films of SP-B/SP-A/(DPPC/PG) (Fig. 3 *B*) and SP-C/SP-A/(DPPC/PG) (Fig. 4 *B*) was not reflected in their phase properties determined as a relative proportion of LC phase at a given surface pressure. However, analysis of the number and size of LC domains per frame at  $\pi = 20$  mN/m revealed that fewer LC domains of larger size were formed in the films of SP-B/SP-A/(DPPC/PG) (*double arrowheads* in Fig. 3 *Bc*) compared to the monolayers of SP-C/SP-A/(DPPC/PG) (*double arrowheads* in Fig. 4 *Bc*) (data not shown).

Because the property of proteins to inhibit condensed domain growth and to favor the production of a larger number of smaller domains at the expense of a small number of big domains is concentration-dependent (Heckl et al., 1989; Pérez-Gil et al., 1992; Nag et al., 1997), the latter observation would be consistent with an effectively lower concentration of total protein intermixed with the lipid in the films of SP-B/SP-A/(DPPC/PG) compared to those of SP-C/SP-A/(DPPC/PG). As was discussed at  $\pi = 20$  mN/m each of the films of SP-B/(DPPC/PG) and SP-C/(DPPC/PG) spread on SP-A contained  $\sim 12$  wt % SP-A and, therefore, the differences in the size and number of LC domains seen in the films of SP-B/SP-A/(DPPC/PG) and SP-C/SP-A/(DPPC/PG) were not related to different amounts of SP-A adsorbed in the films.

The films of SP-B/SP-A/(DPPC/PG) and SP-C/SP-A/(DPPC/PG) contained equal weight (though not molar amounts) of each hydrophobic protein, and in the absence of SP-A in the subphase, the phase distribution in the films of DPPC/PG plus either 17 wt % SP-B or SP-C showed the occurrence of a similar number of LC domains of comparable sizes (data not shown). Therefore, the observation that in the presence of SP-A fewer domains of larger size were seen in the films of SP-B/(DPPC/PG) compared to the films of SP-C/(DPPC/PG) could be explained by a strong association of SP-A with SP-B in the SP-B/(DPPC/PG) films, which might have caused the segregation of a SP-A/SP-B from the lipid, and hence produced a protein-depleted lipid phase that was effectively less perturbed by the proteins compared to the lipid in the SP-C/SP-A/(DPPC/PG) films. SP-C and SP-A were likely more uniformly distributed in the lipid LE phase in the latter films. Such a mechanism of SP-A/SP-B interactions may also accommodate the observation of the large probe-excluding aggregates in the lipid

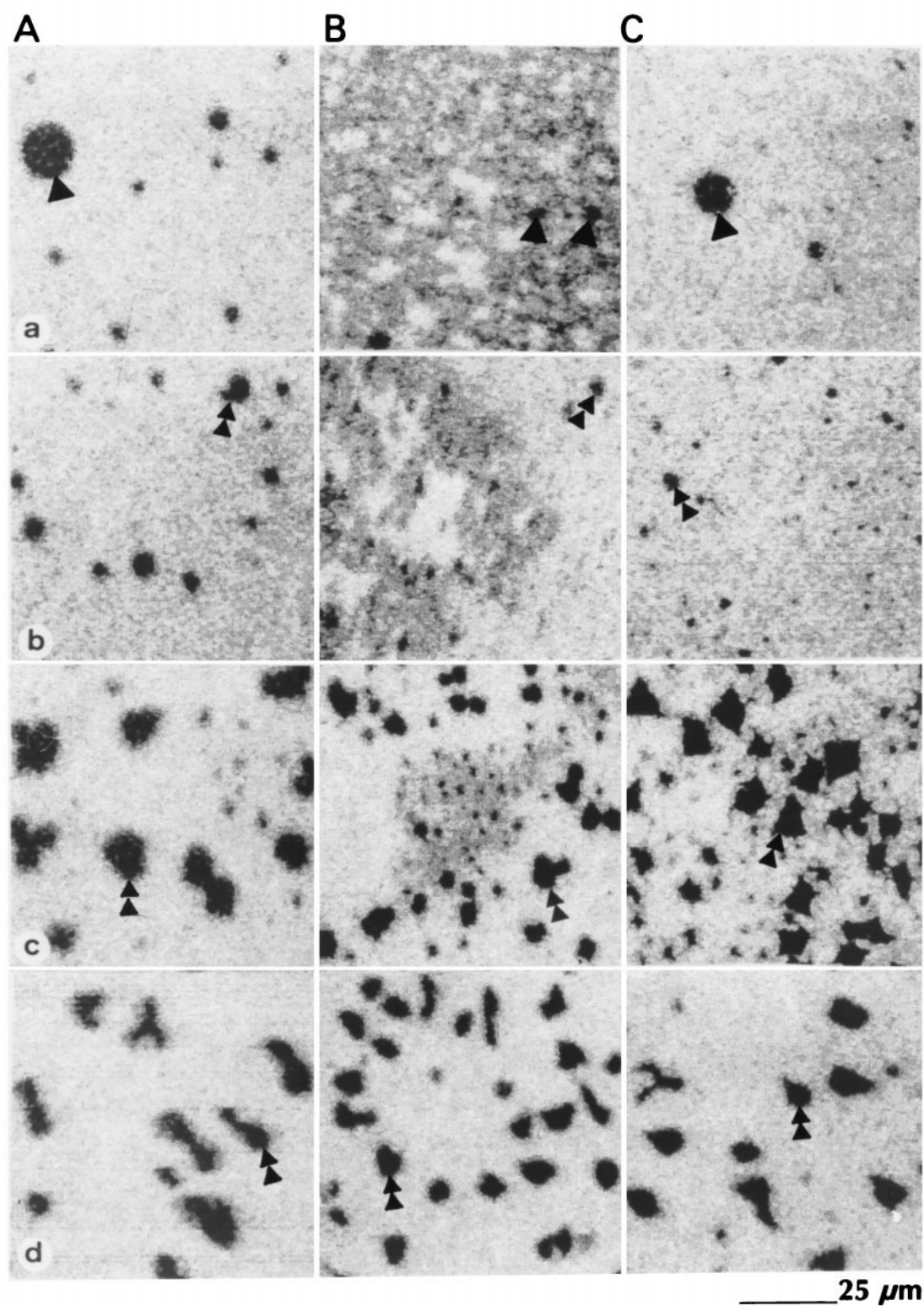


FIGURE 4 Epifluorescence micrographs of monolayers of DPPC/PG (8:2, mol/mol) plus 17 wt % SP-C ( $X_r = 0.56$ ) at a surface pressure of 5 mN/m (a), 10 mN/m (b), 20 mN/m (c), and 35 mN/m (d). The subphase was 145 mM NaCl, 5 mM Tris-HCl (pH 6.9) plus 2 mM EDTA (A); plus 2 mM EDTA and 0.68  $\mu\text{g/ml}$  (B); plus 5 mM  $\text{CaCl}_2$  and 0.68  $\mu\text{g/ml}$  SP-A (C). Single arrowheads indicate gaseous phase and double arrowheads indicate LC domains.

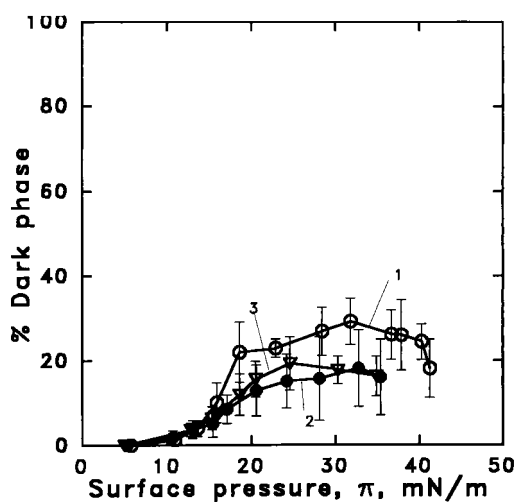


FIGURE 5 Area occupied by LC regions (% dark phase) as a function of surface pressure in monolayers of DPPC/PG (1), DPPC/PG plus 17 wt % SP-B (2), or SP-C (3) spread on subphases of 145 mM NaCl, 5 mM Tris-HCl, 2 mM EDTA, and 0.68  $\mu\text{g/ml}$  SP-A (pH 6.9). Error bars indicate mean  $\pm$  SD for 10 images analyzed at each surface pressure. Percent dark phase does not include the area occupied by the probe-excluding, likely protein-rich, clusters (large arrowheads in Fig. 3 B).

films containing SP-B/SP-A (large arrowheads in Fig. 3 B) compared to the relatively uniform surface textures of the films containing SP-C/SP-A (Fig. 4 B).

In summary, SP-A appeared to insert and produce similar increases in monolayer areas of films of DPPC/PG alone or supplemented with SP-B or SP-C (Fig. 1). Adsorption of SP-A to the lipid or lipid-protein films caused the appearance of a probe-excluding phase different from the conventional lipid probe-excluding LC phase (Figs. 2 B, 3 B, and 4 B). The films of SP-B/SP-A/(DPPC/PG) and SP-C/SP-A/(DPPC/PG) had similar phase properties in terms of percent dark (LC) phase but displayed different morphologies. Preferential interactions of SP-A with SP-B and a separation of a SP-B/SP-A phase may account for the formation of a distinct probe-excluding phase in the lipid films containing SP-B/SP-A (large arrowheads in Fig. 4 B).

### Influence of calcium ions on surface textures of monolayers of DPPC/PG plus SP-B or SP-C spread on subphases containing SP-A

The experiments were performed in the presence of 5 mM  $\text{CaCl}_2$  in the subphase. A threshold concentration of 0.5 mM  $\text{Ca}^{2+}$  has been reported to induce self-association of porcine SP-A, whereas at 1.6 mM  $\text{Ca}^{2+}$ , a level of calcium ions reported for the alveolar subphase of adult rabbit lungs (Nielson, 1984), SP-A was only partially aggregated; the process of self-aggregation of SP-A was completed at  $\sim 5$  mM  $\text{Ca}^{2+}$  (Ruano et al., 1996).

Fig. 6 shows compression isotherms for monolayers of

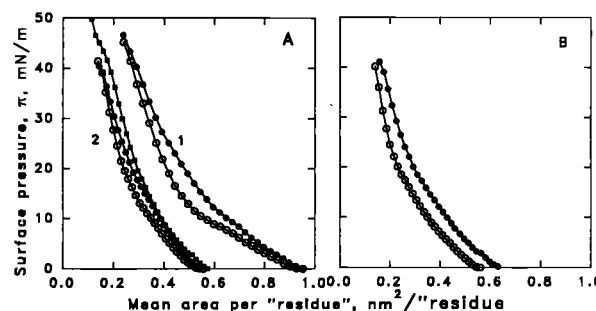


FIGURE 6 Surface pressure as a function of mean area per "residue" for monolayers of (A) DPPC/PG (8:2, mol/mol) (1) and DPPC/PG plus 17 wt % SP-B ( $X_r = 0.58$ ) (2); (B) DPPC/PG plus 17 wt % SP-C ( $X_r = 0.56$ ). Each monolayer contained 1 mol % (based on phospholipid content) of NBD-PC. Subphase was 145 mM NaCl, 5 mM Tris-HCl, 5 mM  $\text{CaCl}_2$  (pH 6.9) without (○) or with (●) 0.68  $\mu\text{g/ml}$  SP-A. Isotherm for films of DPPC/PG plus 17 wt % SP-B spread on 145 mM NaCl, 5 mM Tris-HCl, 5 mM  $\text{CaCl}_2$ , and 0.68  $\mu\text{g/ml}$  con A (■).

DPPC/PG (curve 1, Fig. 6 A) and DPPC/PG plus 17 wt % SP-B (curve 2, Fig. 6 A) or SP-C (Fig. 6 B) spread on calcium-containing subphases in the absence (open circles) or presence (filled circles) of SP-A. Each of the pairs of isotherms ( $\pm$ SP-A) measured in the presence of calcium in the subphase (Fig. 6) was shifted toward lower areas compared to the respective pair obtained in the absence of calcium (Fig. 1); the effect being more pronounced for the films of DPPC/PG without hydrophobic protein. This observation was consistent with the ability of the divalent ions to bind phosphatidylglycerol headgroups and to increase the molecular packing in monolayers containing the negatively charged phospholipid (El Mashak et al., 1982). In the presence of SP-A (filled circles) the nominal area per "residue" was greater than in the absence of SP-A (open circles). This occurs in both the presence and absence of calcium.

Images seen at selected surface pressures in the films of DPPC/PG spread on SP-A solutions in the presence of  $\text{Ca}^{2+}$  in the subphase are shown in Fig. 2 C. Small probe-excluding particles separated from the LE phase at low surface pressures (Fig. 2 Ca). At similar surface pressures monolayers of DPPC/PG were homogeneous when spread on SP-A-free subphases containing 5 mM  $\text{Ca}^{2+}$  (data not shown) or on solutions of SP-A without  $\text{Ca}^{2+}$  (Fig. 2 Ba). Because calcium ions at mM levels induce self-aggregation and alter the quaternary structure of SP-A (Haagsman et al., 1990; Ruano et al., 1996; Palaniyar et al., 1998), it could be assumed that the probe-excluding particles seen at low pressures in the films of DPPC/PG spread on SP-A were likely  $\text{Ca}^{2+}$ -induced aggregates of SP-A adsorbed and likely inserted in the lipid monolayer. At  $\pi \approx 7$  mN/m new probe-excluding domains, likely comprising phospholipid in the LC phase, appeared and grew with increasing surface pressure (double arrowheads in Fig. 2, Cb, c). Interestingly, the protein aggregates cross-linked the lipid LC domains



and formed SP-A-lipid complexes. At  $\pi \geq 25$  mN/m the probe-excluding, likely comprising SP-A, particles that interconnected the LC domains started to lose intensity (Fig. 2 *Cd*).

Fig. 3 *C* shows micrographs of monolayers of SP-B/(DPPC/PG) spread on subphases of SP-A plus calcium. The features of the films were similar to those seen in their counterparts at corresponding surface pressures in the absence of  $\text{Ca}^{2+}$  (Fig. 3 *B*), a result indicating that potential SP-B/SP-A interactions causing the segregation of a protein-rich phase were apparently calcium-independent. The large clusters of probe-excluding phase (*large arrowheads* in Fig. 3, *Ca-d*), which appeared at low surface pressures and occupied  $47\% \pm 18\%$  of the total monolayer surface at  $\pi = 2.5$  mN/m, persisted to the highest surface pressures measured in the films ( $\sim 40$  mN/m).

Contrary to this observation, the surface textures seen in the films of SP-C/(DPPC/PG) spread on SP-A solutions were affected by  $\text{Ca}^{2+}$  (compare Fig. 4, *B* and *C*). In the presence of  $\text{Ca}^{2+}$ , at low surface pressures circular probe-excluding domains, likely representing a protein-stabilized gaseous phase trapped in the LE phase, were dispersed into a fluorescent background (*small arrowheads* in Fig. 4 *Ca*). LC probe-excluding domains of irregular shapes appeared at  $\pi \approx 8$  mN/m and grew with increasing surface pressure (*double arrowheads* in Fig. 4, *Cb, c*). These observations indicated that the films of SP-C/(DPPC/PG) spread on subphases containing SP-A plus  $\text{Ca}^{2+}$  did not show any specific surface organization; they were characterized with surface phases similar to those seen in the films formed on SP-A-free subphases (Fig. 4 *A*). However, in the eyepiece of the microscope the LE phase in the films of SP-C/(DPPC/PG) spread on SP-A appeared grainy and grayish compared to the brightly fluorescent LE phase seen in the films spread on subphases without SP-A, an observation that may be accounted for by  $\text{Ca}^{2+}$ -induced aggregation of SP-A.

The relative area of the probe-excluding LC regions (*double arrowheads* in Figs. 2 *C*, 3 *C*, and 4 *C*) seen via the fluorescence of NBD-PC in the monolayers of DPPC/PG  $\pm$  SP-B or SP-C spread on subphases containing SP-A plus  $\text{Ca}^{2+}$  are plotted in Fig. 7. Note that the surface occupied by the probe-excluding clusters seen in the films of SP-B/SP-A/(DPPC/PG) (*large arrowheads* in Fig. 3 *C*) were excluded from the values of percent dark phase, whereas the areas taken by the probe-excluding aggregates of SP-A (Fig. 2 *C*) and the circular probe-excluding domains in Fig. 4 *C* (*small arrowheads*) were included in percent dark phase at  $5 \text{ mN/m} < \pi \leq 20 \text{ mN/m}$  because similarities in the sizes of the latter structures and those of the LC domains made their distinction difficult. Comparison of the plots of percent dark phase as a function of  $\pi$  for films of DPPC/PG spread on SP-A in the absence and presence of calcium ions (*curves 1* in Figs. 5 and 7, respectively) showed that the divalent ions increased the relative area occupied by the LC phase in the films at  $\pi \leq 30$  mN/m. A similar  $\text{Ca}^{2+}$ -induced

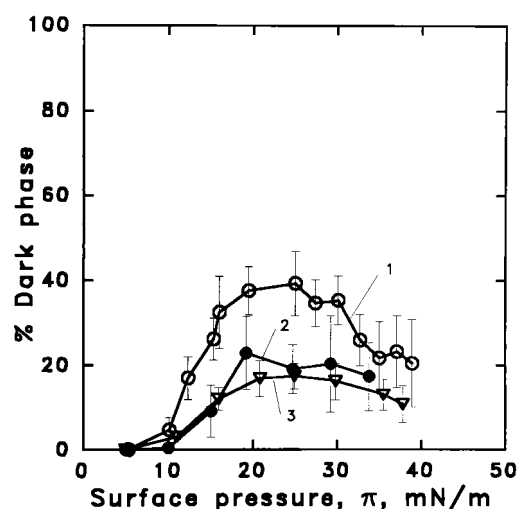


FIGURE 7 Percent dark phase as a function of surface pressure in monolayers of DPPC/PG (1), DPPC/PG plus 17 wt % SP-B (2), or SP-C (3) spread on subphases of 145 mM NaCl, 5 mM Tris-HCl, 5 mM  $\text{CaCl}_2$  and 0.68  $\mu\text{g/ml}$  SP-A (pH 6.9). Error bars indicate mean  $\pm$  SD for 10 images analyzed at each surface pressure. Percent dark phase does not include the area occupied by the probe-excluding, likely protein-rich, clusters (*large arrowheads* in Fig. 3 *C*).

condensation in phospholipid mixtures containing DPPG has been reported previously (Nag et al., 1994). A tendency of  $\text{Ca}^{2+}$  to increase the area covered by the LC phase was also seen in the films of DPPC/PG that contained SP-B/SP-A or SP-C/SP-A (compare *curves 2* and *3* in Fig. 7 to *curves 2* and *3* in Fig. 5); the changes in percent dark phase induced by calcium ions in the latter cases, however, were small and within the variabilities of determinations. The relative proportion of percent dark phase for the films of DPPC/PG, and to a lesser extent for those containing SP-B or SP-C, decreased at  $\sim \pi > 30$  mN/m. As was discussed earlier, some phospholipid from the LC phase likely accompanied the exclusion of components exhibiting low collapse pressures and led to a decrease in the relative amount of the LC phase. The similarity in the plots of percent dark phase ( $\pi$ ) for the two lipid-protein systems (*curves 2* and *3* in Fig. 7) implied that the considerable reorganization in the surface texture and the formation of the probe-excluding clusters (*large arrowheads* in Fig. 3 *C*) in the films that contained SP-B/SP-A did not significantly alter the relative areas occupied by the LC phase compared to the films containing SP-C/SP-A. It is worth noting that the percent dark phase was determined as a relative proportion of the LC domains assuming that the rest of the surface was occupied by probe-including LE phase. However, the physical state of the large probe-excluding clusters seen in the films of SP-B/SP-A/(DPPC/PG) remains unknown. As was discussed, this phase was likely enriched in SP-B/SP-A and may also contain some phospholipid.

In summary, the addition of calcium ions to the subphase did not significantly affect the extent of incorporation of

SP-A into the films of SP-B/(DPPC/PG) or SP-C/(DPPC/PG), or their phase properties defined as percent dark (LC) phase. Likewise, the divalent cations did not significantly alter the surface morphology of the films of SP-B/SP-A/(DPPC/PG), which was consistent with  $\text{Ca}^{2+}$ -independent segregation of a potentially SP-B/SP-A-enriched phase. In the presence of calcium the probe-excluding, likely SP-A-rich, phase seen in the films of DPPC/PG and SP-C/(DPPC/PG) spread on SP-A in the absence of calcium was absent, and possibly  $\text{Ca}^{2+}$ -induced aggregates of SP-A appeared in these films.

### Effects of relative concentrations of SP-A and SP-B on the surface textures of SP-B/(DPPC/PG) films spread on subphases containing SP-A plus $\text{Ca}^{2+}$

The fluorescence micrographs shown in Fig. 3, *B* and *C* revealed that SP-A and SP-B, when present in the DPPC/PG films, produced a characteristic probe-excluding phase that was not seen in the phospholipid films containing either SP-A (Fig. 2 *C*) or SP-B (Fig. 3 *A*) alone. It is likely that strong enough association between SP-B and SP-A overwhelmed interactions between SP-B and the lipid, and thus allowed the segregation of a SP-B/SP-A-enriched phase from the rest of the lipid matrix. This hypothesis was indirectly tested by studying effects of the concentration of either SP-A or SP-B on the appearance of the SP-B/SP-A/(DPPC/PG) films observed through the fluorescence of the lipid probe NBD-PC. Fig. 8 *A* shows data for films of SP-B/(DPPC/PG) that contained 3 wt % SP-B spread on solutions of SP-A at  $C_s = 0.68 \mu\text{g/ml}$ . Similar to the lipid/protein films that contained 17 wt % SP-B (Fig. 3 *C*), probe-excluding aggregates were seen at low  $\pi$  (*large arrowheads* in Fig. 8, *Aa–c*); they coexisted with the lipid LE and LC phases and were still visible at  $\pi = 30 \text{ mN/m}$ . These probe-excluding clusters occupied a smaller surface area compared to the large probe-excluding clusters seen in the films that contained 17 wt % SP-B (*large arrowheads* in Fig. 3 *C*).

In separate experiments, films of SP-B/(DPPC/PG) containing 17 wt % SP-B were spread on solutions that contained SP-A at  $C_s = 0.24 \mu\text{g/ml}$ , and their fluorescence micrographs (Fig. 8 *B*) were compared to the micrographs taken of their counterparts spread on SP-A solutions at  $C_s = 0.68 \mu\text{g/ml}$  (Fig. 3 *C*). Probe-excluding clusters were observed in the films spread on solutions of SP-A at low concentration (*large arrowheads* in Fig. 8 *B*); however, they occupied a smaller proportion from the monolayer surface compared to that in the films formed on SP-A solution containing higher levels of SP-A (Fig. 3 *C*).

In summary, the correlation between the area taken by the probe-excluding clusters seen in the monolayers of DPPC/PG plus SP-A/SP-B and the level of each protein in the lipid-protein films implied that the two proteins controlled the formation of this phase.

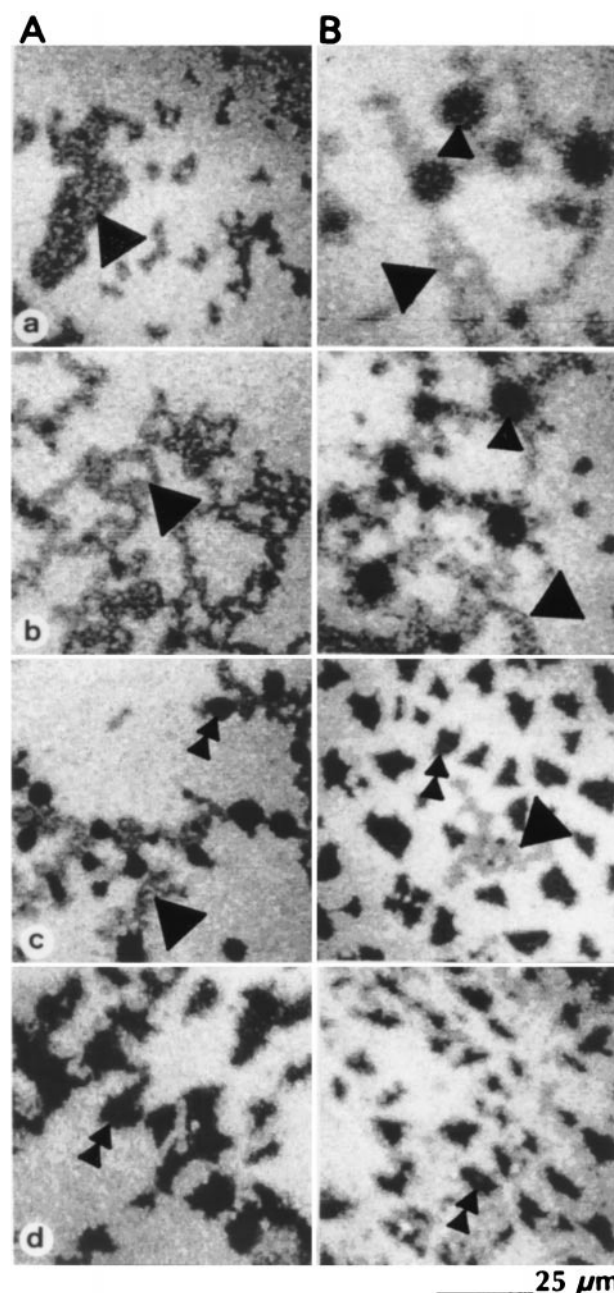


FIGURE 8 Epifluorescence micrographs at selected surface pressures of 5 mN/m (*a*), 10 mN/m (*b*), 20 mN/m (*c*), and 35 mN/m (*d*) of monolayers of DPPC/PG (8:2, mol/mol) plus 3 wt % SP-B ( $X_r = 0.17$ ) spread on 145 mM NaCl, 5 mM Tris-HCl, 5 mM  $\text{CaCl}_2$  plus 0.68  $\mu\text{g/ml}$  SP-A (*A*); DPPC/PG plus 17 wt % SP-B ( $X_r = 0.58$ ) spread on 145 mM NaCl, 5 mM Tris-HCl, 5 mM  $\text{CaCl}_2$  plus 0.24  $\mu\text{g/ml}$  SP-A (*B*). Small arrowheads indicate gaseous phase, double arrowheads LC domains, and large arrowheads SP-A/SP-B-rich phase.

### Surface morphologies of monolayers of DPPC/PG plus a mixture of SP-B and SP-C spread on subphases containing SP-A

Micrographs of monolayers of DPPC/PG plus 17.4 wt % SP-B/SP-C (1:2, wt/wt, a ratio corresponding to the rela-



tionship between the amounts of the two purified proteins) spread on solutions of SP-A ( $C_s = 0.68 \mu\text{g/ml}$ ) in the absence or presence of calcium ions are shown in Fig. 9, *A* and *B*. These films, which contained higher concentrations of SP-C (11.7 wt %) than SP-B (5.7 wt %), acquired appearances analogous to those seen in the films of

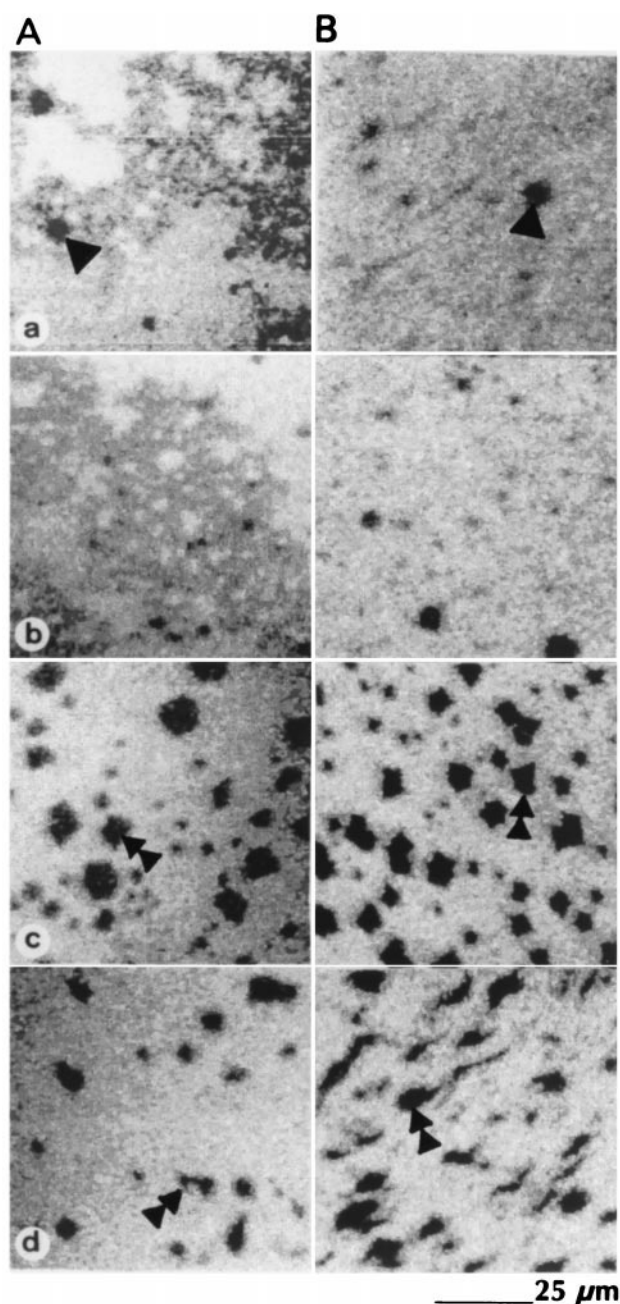


FIGURE 9 Epifluorescence images at selected surface pressures of 5 mN/m (*a*), 10 mN/m (*b*), 20 mN/m (*c*), and 35 mN/m (*d*) of monolayers of DPPC/PG (8:2 mol/mol) plus 17 wt % SP-B/SP-C (1:2 wt/wt) spread on 145 mM NaCl, 5 mM Tris-HCl, 0.68  $\mu\text{g/ml}$  SP-A plus 2 mM EDTA (*A*) or 5 mM  $\text{CaCl}_2$  (*B*). Single arrowheads indicate gaseous phase and double arrowheads indicate LC domains.

DPPC/PG plus 17 wt % SP-C in the absence or presence of  $\text{Ca}^{2+}$  (Fig. 4, *B* and *C*, respectively). A grayish probe-excluding phase was seen at  $2.5 \text{ mN/m} \leq \pi \leq 20 \text{ mN/m}$  in the films of DPPC/PG containing the three surfactant proteins in the absence of calcium in the subphase (Fig. 9 *A*). In the presence of calcium no surface structures, additional to the probe-excluding circular gaseous domains (arrowheads in Fig. 9 *Ba*) or the lipid LC domains (double arrowheads in Fig. 9, *Bc, d*), were seen at any surface pressure (Fig. 9 *B*). However, the fluorescent background looked grainy and grayish. Under these conditions a separate probe-excluding phase distinctive for the combined presence of SP-B/SP-A without SP-C was not observed. Interestingly, in the absence of SP-C the films of DPPC/PG that contained 3 wt % SP-B, a concentration lower than the level of SP-B in the lipid films plus SP-B/SP-C spread on SP-A, exhibited elements characteristic for the SP-A/SP-B separated phase (large arrowheads in Fig. 8 *A*). This observation implied that interactions between SP-A and SP-B likely could not cause the removal of SP-B from its intimate mixture with SP-C and the phospholipids. Such an explanation is consistent with previous findings that SP-B and SP-C mixed ideally in binary monolayers of SP-B/SP-C (Taneva and Keough, 1994b) and both partitioned into the LE phase in films of SP-B/SP-C plus DPPC (Nag et al., 1997).

In summary, the surface morphologies of lipid monolayers containing the combination of SP-B/SP-C (1:2, wt/wt) spread on SP-A were determined by interactions of SP-A with the prevailing SP-C.

#### Effects of concanavalin A on surface textures of films of DPPC/PG plus SP-B

To determine whether the surface morphologies imparted by SP-A to the films of SP-B/(DPPC/PG) were specific to this protein, SP-A was replaced with con A at the same subphase concentration. Con A, which lacks covalently bound carbohydrates, is a member of the lectin family of plant proteins; it has binding sites for calcium ions and saccharides. Equilibrium surface pressure (surface tension change) of  $2.1 \pm 0.5 \text{ mN/m}$  was measured for solutions of con A at  $C_s = 0.68 \mu\text{g/ml}$  (145 mM NaCl, 5 mM Tris-HCl, 5 mM  $\text{CaCl}_2$ ), whereas under similar experimental conditions and concentration a surface pressure of  $4 \pm 1 \text{ mN/m}$  was measured for SP-A. The isotherm for monolayers of SP-B/(DPPC/PG) spread on subphases containing con A (filled squares in Fig. 6 *A*) was shifted to higher molecular areas compared to the isotherm of the lipid-protein films spread on protein-free subphases (open circles in Fig. 6 *A*). The result suggested that con A at this subphase concentration inserted into the spread films of SP-B/(DPPC/PG) and caused an increase in the mean area per “residue” comparable to that induced by SP-A at the same concentration (filled circles in Fig. 6 *A*). The two water-soluble proteins, which exhibited commensurate activities in their adsorption



to the monolayer-free or monolayer-covered surfaces, imparted considerably different morphologies to the SP-B/(DPPC/PG) films (compare Figs. 3 C and 10). A number of probe-excluding structures were seen in the films of SP-B/(DPPC/PG) spread on con A: circular domains likely comprising a gaseous phase (*small arrowheads* in Fig. 10 a); LC domains (*double arrowheads* in Fig. 10, b–d); and large patches, likely consisting of con A aggregated at the surface, seen infrequently in the films at all surface pressures studied (*arrows* in Fig. 10, b–d). Similar textures were seen in films of SP-B/(DPPC/PG) that were spread on subphases containing con A at  $C_s = 1.26 \mu\text{g/ml}$  (data not shown). Epifluorescence microscopy on films of DPPC/DPPG spread on subphases containing either SP-A or con A without  $\text{Ca}^{2+}$  has demonstrated that in the absence of hydrophobic protein in the spread lipid films both SP-A and con A aggregated and accumulated at the LE/LC boundaries of the lipid-condensed domains (Ruano et al., 1998). These data, taken together with the differences observed in the textures of SP-B/(DPPC/PG) films spread on SP-A and con A, suggested that specific interactions between SP-A and SP-B in the monolayers likely determined the morphologies of the quaternary SP-B/SP-A/(DPPC/PG) films.

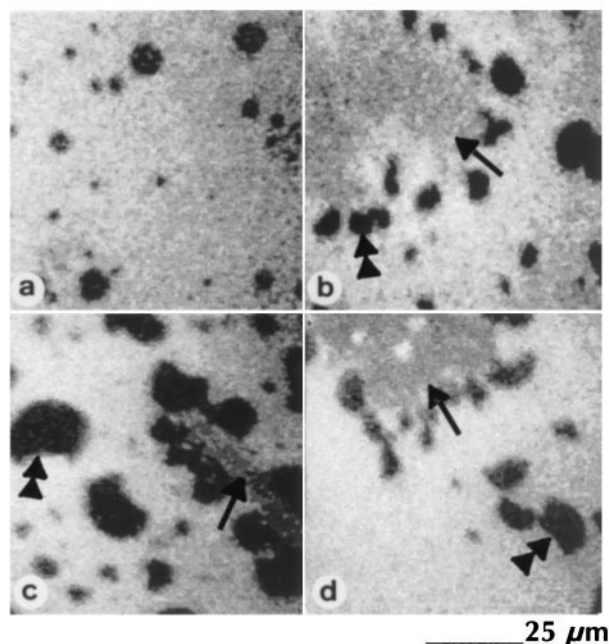


FIGURE 10 Epifluorescence images at a surface pressure of 5 mN/m (a), 10 mN/m (b), 20 mN/m (c), and 35 mN/m (d) of monolayers of DPPC/PG (8:2, mol/mol) plus 17 wt % SP-B ( $X_r = 0.58$ ) spread on 145 mM NaCl, 5 mM Tris-HCl, 5 mM  $\text{CaCl}_2$  plus  $0.68 \mu\text{g/ml}$  con A. Small arrowheads indicate gaseous phase, double arrowheads LC domains, and arrows indicate patches of con A seen infrequently in the films.

## DISCUSSION AND CONCLUSIONS

The main observation in the present study was that SP-A induced striking changes in the surface morphology of SP-B/(DPPC/PG) monolayers. A probe-excluding surface phase unique for the phospholipid films containing SP-A/SP-B required the presence of the two proteins and depended on the lipid-to-protein stoichiometry. This phase was seen in the monolayers of SP-B/SP-A/(DPPC/PG) regardless of the presence of calcium in the subphase, and this finding implied that potential  $\text{Ca}^{2+}$ -induced self-aggregation of SP-A did not alter its interactions with SP-B in the lipid films. SP-C could not replace SP-B and con A could not substitute for SP-A in the properties of the pair of SP-B/SP-A to produce the distinctive probe-excluding phase. In the absence of calcium in the subphase SP-A adsorbed to the LE phase in monolayers of DPPC/PG alone or supplemented with SP-C, and caused the formation of a probe-excluding phase different from the probe-excluding lipid LC phase. The addition of calcium ions eliminated the probe-excluding phase that covered parts of the monolayer surface and was associated with adsorption of SP-A, and caused the appearance of tiny probe-excluding particles, likely consisting of aggregated SP-A, which were aligned around the LE/LC phase in the DPPC/PG and distributed in the LE phase of SP-C/(DPPC/PG) monolayers. Analysis of the monolayer areas in the films of SP-B/(DPPC/PG) and SP-C/(DPPC/PG) formed in the presence and absence of SP-A in the subphase indicated that similar amounts of SP-A were incorporated in the two lipid-protein systems. In agreement with this observation, these systems displayed similar properties in terms of surface pressure-area characteristics and percentage of area occupied by the LC phase. Therefore, the differences seen in the SP-A-induced morphologies of the films of SP-B/(DPPC/PG) and SP-C/(DPPC/PG) were not a consequence of the extent to which SP-A was incorporated in the lipid-protein films. Rather, they could be attributed to the ability of SP-A to laterally redistribute SP-B but not SP-C, both of which occupy the lipid LE phase in the absence of SP-A in the subphase (Nag et al., 1997). It is noteworthy that the distributions of SP-B and SP-C in the protein-lipid monolayers spread on SP-A would depend on the balance of the interactions of each hydrophobic protein with SP-A and with the lipid. Plots of the mean area per “residue” as a function of the monolayer composition for the monolayers of SP-B/(DPPC/PG) and SP-C/(DPPC/PG) in the absence of SP-A in the subphase showed additivity suggesting similar protein-lipid interactions in the two systems.

We have not found a substantial role for calcium ions in the interactions of SP-A with the lipid or protein-lipid monolayers. The divalent cation did not substantially affect the morphology of the SP-B/SP-A/(DPPC/PG) films. The surface features of the films of DPPC/PG and SP-C/(DPPC/PG) spread on SP-A were affected by  $\text{Ca}^{2+}$ . In these latter

two systems, at low pressure when calcium was present, the fields showed a fairly uniform distribution of tiny aggregates that had grey appearance. When calcium was absent from either DPPC/PG or SP-C/(DPPC/PG) monolayers spread over SP-A, these grey aggregates displayed a network arrangement (Figs. 2 B and 4 B). The amounts of SP-A estimated to be incorporated into the films of DPPC/PG alone or supplemented with SP-B or SP-C appeared to be similar in the presence and absence of calcium in the subphase. Some studies have indicated calcium-independent binding of SP-A to phospholipid membranes (King et al., 1983; Casals et al., 1993; Poulain et al., 1996), whereas others have demonstrated a requirement for calcium in aggregation of phospholipid vesicles (Haagsman et al., 1987; Poulain et al., 1992) and formation of tubular myelin in vitro (Suzuki et al., 1989; Williams et al., 1991) and in vivo (Benson et al., 1984). Calcium ions likely were not required for the intimate molecular interactions of SP-A with the lipid membranes; however, in the latter experiments, they were necessary to modify the charge and hydration states of adjacent bilayers that had to come to close proximity for the properties displayed in those studies.

Lattice structures typical of tubular myelin have been detected in the presence of ~17 wt % SP-B and 20 wt % SP-A in mixtures of DPPC and PG (Suzuki et al., 1989; Williams et al., 1991). The monolayer experiments reported here also revealed a positive correlation of the levels of SP-A and SP-B with the amount of the characteristic probe-excluding phase seen in the films of SP-B/(DPPC/PG) spread on SP-A. In the latter mixture high concentrations of SP-B (17 wt %) and SP-A ( $C_s = 0.68 \mu\text{g/ml}$ , a subphase concentration that caused the insertion of ~12 wt % SP-A into the monolayers of SP-B/(DPPC/PG)) were required for the reorganization of the surface textures of the films. An estimation based on data for the composition of pulmonary surfactant subtypes (Putman et al., 1996) showed that the heavy subtype, which includes tubular myelin, contains ~2.5 wt % hydrophobic protein (SP-B and SP-C, where SP-B/SP-C are in the ratio 1:3, wt/wt) and 5.5 wt % SP-A; these protein levels being considerably lower than those required for the assembly of tubular myelin in vitro (Suzuki et al., 1989; Williams et al., 1991). It is likely that most, if not all, of the constituents of the multicomponent system of natural surfactant affect the structural reorganization of pulmonary surfactant in the alveolar subphase, and this may explain why different lipid-protein stoichiometries were required for reconstitution of tubular myelin from only a few components in vitro.

The results from this study are consistent with the possibility of separating an SP-A/SP-B-rich phase that may be involved in the assembly of tubular myelin in vitro and in vivo. Preferential interaction of SP-A with SP-B in lipid membranes and subsequent segregation of an SP-B/SP-A-rich phase may provide loci required for the extensive aggregation and fusion of lipid bilayers to form the tubular

myelin lattice. Such a mechanism of SP-A/SP-B interactions could accommodate a model for tubular myelin where SP-B acts as an integral protein in the lipid and SP-A resides as an extrinsic protein, perhaps associated with the small hydrophilic portion of SP-B (Williams et al., 1991).

The epifluorescence microscopic observations provide evidence for association of SP-A with SP-B and a segregation of an SP-B/SP-A phase in phospholipid membranes. The role of the phospholipid composition on the ability of the combination of SP-A and SP-B to reorganize the surface textures of the lipid-protein monolayers still needs to be elucidated.

This work was supported by the Medical Research Council of Canada.

## REFERENCES

- Bartlett, G. R. 1959. Phosphorus assay in column chromatography. *J. Biol. Chem.* 234:466–468.
- Benson, B. J., M. C. Williams, K. Sueishi, J. Goerke, and T. Sargeant. 1984. Role of calcium ions in the structure and function of pulmonary surfactant. *Biochim. Biophys. Acta.* 793:18–27.
- Boonman, A., F. H. Machiels, A. F. M. Snik, and J. Egbers. 1987. Squeeze-out from mixed monolayers of dipalmitoylphosphatidylcholine and egg phosphatidylglycerol. *J. Colloid Interface Sci.* 120:456–468.
- Casals, C., E. Miguel, and J. Perez-Gil. 1993. Tryptophan fluorescence study on the interaction of pulmonary surfactant protein A with phospholipid vesicles. *Biochem. J.* 296:585–593.
- Clements, J. A., R. F. Hustead, R. P. Johnson, and I. Gribitz. 1961. Pulmonary surface tension and alveolar stability. *J. Appl. Physiol.* 16: 447–450.
- Curstedt, T., J. Johansson, J. Barros-Söderling, B. Robertson, G. Nilsson, M. Westberg, and H. Jörnvall. 1988. Low-molecular-mass surfactant protein type 1. The primary structure of a hydrophobic 8-kDa polypeptide with eight half-cystine residues. *Eur. J. Biochem.* 172:521–525.
- Curstedt, T., J. Johansson, P. Persson, A. Eklund, B. Robertson, B. Löwenadler, and H. Jörnvall. 1990. Hydrophobic surfactant-associated polypeptides: SP-C is a lipopeptide with two palmitoylated cysteine residues, whereas SP-B lacks covalently linked fatty acyl groups. *Proc. Natl. Acad. Sci. USA.* 87:2985–2989.
- El Mashak, E. M., F. Lakhdar-Ghazal, and J. F. Tocanne. 1982. Effect of pH, mono- and divalent cations on the mixing of phosphatidylglycerol with phosphatidylcholine. *Biochim. Biophys. Acta.* 688:465–474.
- Gil, J., and O. K. Reiss. 1973. Isolation and characterization of lamellar bodies and tubular myelin from rat lung homogenates. *J. Cell Biol.* 58:152–171.
- Haagsman, H. P., S. Hawgood, T. Sargeant, D. Buckley, R. T. White, K. Drickamer, and B. J. Benson. 1987. The major lung surfactant protein, SP 28-36, is a calcium dependent, carbohydrate-binding protein. *J. Biol. Chem.* 262:13877–13880.
- Haagsman, H. P., T. Sargeant, P. V. Hauschka, B. J. Benson, and S. Hawgood. 1990. Binding of calcium to SP-A, a surfactant-associated protein. *Biochemistry.* 29:8894–8900.
- Hawgood, S., B. J. Benson, J. Schilling, D. Damm, J. A. Clements, and R. Tyler White. 1987. Nucleotide and amino acid sequences of pulmonary surfactant protein SP 18 and evidence for cooperation between SP 18 and SP 28-36 in surfactant lipid adsorption. *Proc. Natl. Acad. Sci. USA.* 84:66–70.
- Hawgood, S., H. Efrati, J. Schilling, and B. J. Benson. 1985. Chemical characterization of lung surfactant apoproteins: amino acid composition. N-terminal sequence and enzymic digestion. *Biochem. Soc. Trans.* 13: 1092–1096.
- Heckl, W. M., M. Thompson, and H. Möhwald. 1989. Fluorescence and electron microscopic study of lectin-polysaccharide and immunochemi-

- cal aggregation at phospholipid Langmuir-Blodgett monolayers. *Langmuir*. 390:390–394.
- Keough, K. M. W., and N. Kariel. 1987. Differential scanning calorimetric studies of aqueous dispersions of phosphatidylcholines containing two polyenoic chains. *Biochim. Biophys. Acta*. 902:11–18.
- King, R. J., and J. A. Clements. 1972. Surface active material from dog lung. I. Method of isolation. *Am. J. Physiol.* 223:707–714.
- King, R. J., M. C. Carmichael, and P. M. Horowitz. 1983. Reassembly of lipid-protein complexes of pulmonary surfactant. *J. Biol. Chem.* 258:10672–10680.
- King, R. J., D. Simon, and P. M. Horowitz. 1989. Aspects of secondary and quaternary structure of surfactant protein A from canine lung. *Biochim. Biophys. Acta*. 1001:294–301.
- Laemmli, U. K. 1970. Cleavage of structural proteins during the assembly of the head of bacteriophage T<sub>4</sub>. *Nature*. 227:680–685.
- Nag, K., C. Boland, N. Rich, and K. M. W. Keough. 1990. Design and construction of an epifluorescence microscopic surface balance for the study of lipid monolayer phase transitions. *Rev. Sci. Instrum.* 61:3425–3430.
- Nag, K., N. H. Rich, C. Boland, and K. M. W. Keough. 1991. Epifluorescence microscopic observation of monolayers of dipalmitoylphosphatidylcholine: dependence of domain size on compression rates. *Biochim. Biophys. Acta*. 1068:157–160.
- Nag, K., N. H. Rich, and K. M. W. Keough. 1994. Interaction between dipalmitoylphosphatidylglycerol and phosphatidylcholine and calcium. *Thin Solid Films*. 244:841–844.
- Nag, K., S. Taneva, J. Pérez-Gil, A. Cruz, and K. M. W. Keough. 1997. Combinations of fluorescently labeled pulmonary surfactant proteins SP-B and SP-C in phospholipid films. *Biophys. J.* 72:2638–2650.
- Nielson, D. W. 1984. Ca<sup>++</sup> activity in the alveolar subphase. *Pediatr. Res.* 17:386a. (Abstr).
- Palaniyar, H., R. A. Ridsdale, C. E. Holterman, K. Inchley, F. Possmayer, and G. Harauz. 1998. Structural changes of surfactant protein A induced by cations reorient the protein on lipid bilayers. *J. Struct. Biol.* 122:297–310.
- Pérez-Gil, J., K. Nag, S. Taneva, and K. M. W. Keough. 1992. Pulmonary surfactant protein SP-C causes packing rearrangements of dipalmitoylphosphatidylcholine in spread monolayers. *Biophys. J.* 63:197–204.
- Poulain, F. R., L. Allen, M. C. Williams, R. L. Hamilton, and S. Hawgood. 1992. Effects of surfactant apolipoproteins on liposome structure: implications for tubular myelin formation. *Am. J. Physiol. Lung Cell Mol. Physiol.* 262:L730–L739.
- Poulain, F. R., S. Nir, and S. Hawgood. 1996. Kinetics of phospholipid membrane fusion induced by surfactant apoproteins A and B. *Biochim. Biophys. Acta*. 1278:169–175.
- Putman, E., L. A. J. M. Creuwels, L. M. G. van Golde, and H. P. Haagsman. 1996. Surface properties, morphology and protein composition of pulmonary surfactant subtypes. *Biochem. J.* 320:599–605.
- Ruano, M. L. F., E. Miguel, J. Pérez-Gil, and C. Casals. 1996. Comparison of lipid aggregation and self-aggregation activities of pulmonary surfactant-associated protein A. *Biochem. J.* 313:683–689.
- Ruano, M. L. F., K. Nag, L.-A. Worthman, C. Casals, J. Pérez-Gil, and K. M. W. Keough. 1998. Differential partitioning of pulmonary surfactant protein SP-A into regions of monolayers of dipalmitoyl phosphatidylcholine and dipalmitoylphosphatidylcholine/dipalmitoyl phosphatidylglycerol. *Biophys. J.* 74:1101–1109.
- Sarin, V. K., S. Gupta, T. K. Leung, V. E. Taylor, B. L. Ohning, J. A. Whitsett, and J. L. Fox. 1990. Biophysical and biological activity of a synthetic 8.7-kDa hydrophobic pulmonary surfactant protein SP-B. *Proc. Natl. Acad. Sci. USA*. 87:2633–2637.
- Sen, A., S.-W. Hui, M. Mosgrober-Anthony, B. A. Holm, and E. A. Egan. 1988. Localization of lipid exchange sites between bulk lung surfactants and surface monolayer: Freeze fracture study. *J. Colloid Interface Sci.* 126:355–360.
- Sueishi, K., and B. J. Benson. 1981. Isolation of a major apolipoprotein of canine and murine pulmonary surfactant. Biochemical and immunological characteristics. *Biochim. Biophys. Acta*. 665:442–453.
- Suzuki, Y., Y. Fujita, and K. Kogishi. 1989. Reconstitution of tubular myelin from synthetic lipids and proteins associated with pig pulmonary surfactant. *Am. Rev. Respir. Dis.* 140:140:75–81.
- Taneva, S., and K. M. W. Keough. 1994a. Dynamic surface properties of pulmonary surfactant proteins SP-B and SP-C and their mixtures with dipalmitoylphosphatidylcholine. *Biochemistry*. 33:14660–14670.
- Taneva, S., and K. M. W. Keough. 1994b. Pulmonary surfactant proteins SP-B and SP-C in spread monolayers at the air-water interface. III. Proteins SP-B plus SP-C with phospholipids in spread monolayers. *Biophys. J.* 66:1158–1166.
- Taneva, S., and K. M. W. Keough. 1995. Calcium ions and interactions of pulmonary surfactant proteins SP-B and SP-C with phospholipids in spread monolayers at the air/water interface. *Biochim. Biophys. Acta*. 1236:185–195.
- Taneva, S., T. McEachren, J. Stewart, and K. M. W. Keough. 1995. Pulmonary surfactant protein SP-A with phospholipids in spread monolayers at the air-water interface. *Biochemistry*. 34:10279–10289.
- Udenfriend, S., S. Stein, P. Bohlen, W. Dairman, W. Loimgrukes, and M. Weigle. 1972. Fluorescamine: a reagent for assay of amino acids, peptides, and primary amines in the picomole range. *Science*. 178:871–872.
- Venkitaraman, A. R., S. B. Hall, J. A. Whitsett, and R. H. Notter. 1990. Enhancement of biophysical activity of lung surfactant extracts and phospholipid-apoprotein mixtures by surfactant protein A. *Chem. Phys. Lipids*. 56:185–194.
- Von Neergaard, K. 1929. Neue Auffassungen über einen Grundbegriff der Atemmechanik. Die Retraktionskraft der Lunge, Abhängig von der Oberflächenspannung in den Alveolen. *Z. Gesamte Exp. Med.* 66:373–394.
- Walker, S. R., M. C. Williams, and B. Benson. 1986. Immunocytochemical localization of the major surfactant apoproteins in type II cells, clara cells, and alveolar macrophages of rat lungs. *J. Histochem. Cytochem.* 34:1137–1148.
- Williams, M. C., S. Hawgood, and R. L. Hamilton. 1991. Changes in lipid structure produced by surfactant proteins SP-A, SP-B, and SP-C. *Am. J. Respir. Cell Mol. Biol.* 5:41–50.
- Yu, S. H., N. Smith, P. G. R. Harding, and F. Possmayer. 1983. Bovine pulmonary surfactant: Chemical composition and physical properties. *Lipids*. 18:522–529.